Equilibrium Atmospheric Response to North Atlantic SST Anomalies*

YOCHANAN KUSHNIR

Lamont-Doherty Earth Observatory, Columbia University, Palisades, New York

ISAAC M. HELD

Geophysical Fluid Dynamics Laboratory/NOAA, Princeton, New Jersey

(Manuscript received 6 April 1995, in final form 22 September 1995)

ABSTRACT

The equilibrium general circulation model (GCM) response to sea surface temperature (SST) anomalies in the western North Atlantic region is studied. A coarse resolution GCM, with realistic lower boundary conditions including topography and climatological SST distribution, is integrated in perpetual January and perpetual October modes, distinguished from one another by the strength of the midlatitude westerlies. An SST anomaly with a maximum of 4°C is added to the climatological SST distribution of the model with both positive and negative polarity. These anomaly runs are compared to one another, and to a control integration, to determine the atmospheric response. In all cases warming (cooling) of the midlatitude ocean surface yields a warming (cooling) of the atmosphere over and to the east of the SST anomaly center. The atmospheric temperature change is largest near the surface and decreases upward. Consistent with this simple thermal response, the geopotential height field displays a baroclinic response with a shallow anomalous low somewhat downstream from the warm SST anomaly. The equivalent barotropic, downstream response is weak and not robust. To help interpret the results, the realistic GCM integrations are compared with parallel idealized model runs. The idealized model has full physics and a similar horizontal and vertical resolution, but an all-ocean surface with a single, permanent zonal asymmetry. The idealized and realistic versions of the GCM display compatible response patterns that are qualitatively consistent with stationary, linear, quasigeostrophic theory. However, the idealized model response is stronger and more coherent. The differences between the two model response patterns can be reconciled based on the size of the anomaly, the model treatment of cloud–radiation interaction, and the static stability of the model atmosphere in the vicinity of the SST anomaly. Model results are contrasted with other GCM studies and observations.

1. Introduction

The effects of extratropical sea surface temperature (SST) anomalies on the atmospheric circulation remain obscure. This problem has been addressed repeatedly with general circulation models (GCMs), with results that are much less satisfactory than the analogous calculations with tropical SST anomalies. The literature prior to 1985 was reviewed by Frankignoul (1985). More recent results have yet to yield an unambiguous picture. For example:

- The experiment of Lau and Nath (1990), using a spectral model with a rhomboidal truncation at wavenumber 15 (equivalent to a grid resolution of ~4.5° lat × 7.5° long), with observed SST distributions from the years 1950–1979, suggests that extratropical anomalies play a significant role in producing the simulated interannual variability during winter. However, Lau and Nath (1994) were not able to reproduce their earlier results when they used the same GCM but with an added cloud prediction scheme (the earlier model version used prescribed zonally symmetric clouds for that purpose).
- Pitcher et al. (1988) obtain a marked nonlinearity in the response to a typical North Pacific SST anomaly in a perpetual January R15 model. The geopotential response retains the same polarity when the sign of the SST anomaly is reversed. Support for this surprising result was obtained by Kushnir and Lau (1992), who also noted a significant difference between the response during the first 90 days of an ensemble of integrations and the subsequent equilibrated response.
- Palmer and Sun (1985) find a substantial response to a North Atlantic anomaly pattern in a model with uniform horizontal resolution of 330 km. Their model displays a surface high to the east northeast of a warm anomaly. They argue that this response resembles the

* Lamont-Doherty Earth Observatory Contribution Number 5488.

Corresponding author address: Dr. Yochanan Kushnir, Lamont-Doherty Earth Observatory, Columbia University, P.O. Box 1000, Palisades, NY 10964-8000.
E-mail: kushnir@ldeo.columbia.edu

observed atmospheric structure correlated with this SST pattern. Ferranti et al. (1994), who examined the GCM response to both tropical and extratropical SST anomalies, were able to reproduce the results of Palmer and Sun using somewhat different Atlantic SST anomalies. They also present separate figures for the response to positive and negative anomalies that, while weak, are similar but opposite in polarity. Peng et al. (1995) experimented with an SST anomaly similar to Palmer and Sun in a model with similar resolution, and compared the response under both November and January conditions. They find a response qualitatively similar to Palmer and Sun but only in their integrations with November initial conditions. January calculations give just the opposite response, with a low downstream of a warm anomaly. Furthermore, their November response is evidently nonlinear, with only the warm anomaly producing a significant response.

A fundamental difficulty in interpreting these GCM integrations are the inconsistent results they display and the absence of an accepted theoretical framework to shape our expectations. One common denominator among these integrations is that the responses, when significant, are equivalent barotropic. The simplest theory we possess, that of the linear response to extratropical heat sources in a zonally symmetric flow, invariably predicts a baroclinic response in the vicinity of the heat source (e.g., Held 1983). Ting (1991) has shown that this linear, baroclinic response can be clearly seen in a model with zonally symmetric SST, when the zonally symmetric climate is perturbed by a strong localized SST anomaly. Responses in qualitative agreement with linear theory were also obtained in realistic GCM studies forced with very large ($\sim$10°C) North Atlantic SST anomalies in the modeling studies of Rind et al. (1986) and Manabe and Stouffer (1988).

It is natural to hope that models linearized about zonally asymmetric basic states will help one understand GCM responses in which a zonally asymmetric climate is perturbed. These models are known to have the potential for producing equivalent barotropic resonances that could be excited by the localized heating. Barotropic responses can be excited also through forcing of the upper-tropospheric vorticity. Whenever linear models with asymmetric basic states are used to analyze the quasi-stationary characteristics of GCMs, changes in upper-tropospheric eddy vorticity fluxes, associated with storm track displacements, are generally the dominant forcing agent. This has been the case in the study of the extratropical response to tropical SST anomalies by Held et al. (1989) and the study of free atmospheric low-frequency variability by Branstator (1992) and Ting and Lau (1993). One can visualize the extratropical SST anomaly as perturbing a storm track and its associated upper-level vorticity fluxes, with the latter forcing an anomalous equivalent barotropic response. Or perhaps the equivalent barotropic stationary "wave" and the storm track must be considered as inseparable parts of a "coherent structure," which responds to the anomaly. Or one may have to think, not of linear dynamics about some asymmetric state, but of the statistics of preexisting, nonlinear, equivalent barotropic variability as being modified by the perturbed boundary condition (i.e., Molteni et al. 1993).

To approach this complex of issues, we study the response to an SST anomaly in both a realistic GCM and in an idealized GCM with an asymmetric climate. Our study uses a low-resolution, R15 model (roughly 4.5° lat $\times$ 7.5° long) and perpetual insolation. This configuration allows us to define the climatic response clearly with long integrations. We recognize the danger that model deficiencies, particularly those in the representation of baroclinic eddy momentum fluxes in such a model (e.g., Held and Phillipps 1993), could distort the results. These constraints are taken into account in our interpretation of the results. The present model does, however, provide a useful tool to examine other aspects of the midlatitude ocean–atmosphere interaction. Note also that the present model has been frequently used for extended integrations to study climate trends and climate variability, either forced with prescribed SST anomalies or coupled to an ocean GCM (e.g., Lau and Nath 1994; Delworth et al. 1993); it is therefore important to document and understand its sensitivity to midlatitude SST anomalies.

We chose to study the response to an Atlantic anomaly because of the suggestive result of Palmer and Sun (1985) and increasing interest in North Atlantic air–sea interaction (Gordon et al. 1992; Deser and Blackmon 1993; Kushnir 1994). Experiments are performed for both perpetual January and perpetual October insolation and SST climatologies to explore the sensitivity to the strength of the underlying westerly circulation, following Peng et al. (1995). We believe that perpetual integrations are relevant to understand GCM results that were obtained in a simulation with the full annual cycle and allow, in this case, the economic study of the winter time response.

In parallel experiments with an idealized GCM we simplify the setting of the experiment by simplifying the complex zonal asymmetry in the basic climate, and removing effects of ocean–land contrast. The use of an idealized model is inspired, in part, by the work of Ting (1991). Given that the linear baroclinic response about a zonally symmetric flow does explain how an R15 model with zonally symmetric climate responds to an SST anomaly, we ask how asymmetric boundary conditions affect the response.

As described below, the results are disappointing in the sense that all of the models that we examine show a rather weak response. Moreover, the responses found are baroclinic, similar to that in Ting (1991), and not equivalent barotropic as in some of the previous GCM experiments outlined above. This amplifies the difficulty in reconciling the different GCM studies. It may

be that higher-resolution models with stronger baroclinic eddy momentum fluxes and sharper storm tracks are needed to provide a more realistic and consistent simulation of the response to midlatitude SST anomalies. Our results, however, show that a better parameterization of physical processes are also needed to simulate diabatic processes in the midlatitude atmosphere.

We feel that the present results are of interest in that 1) they show that an essentially linear baroclinic response can occur in GCMs with strongly asymmetric climates; 2) they reinforce the impression that equivalent barotropic responses to extratropical SST anomalies are delicate—the representation of planetary wave and storm track dynamics provided by the R15 model being insufficient, at least in the calculations described; and 3) they are relevant to understanding previous and ongoing climate studies with this model.

Before turning to the model results, we pause in section 2 to further discuss the issue of baroclinic versus equivalent barotropic responses, in light of the observed structure of atmospheric covariability with SST on interannual and decadal timescales. In particular, Kushnir (1994) has suggested that the atmospheric variability observed on decadal scales might be similar to the linear baroclinic predictions, and we discuss this claim. The idealized and realistic GCM responses are then described in sections 3 and 4.

2. Baroclinic versus barotropic near-field responses

a. Observational studies

Observations indicate that wintertime monthly and seasonal SST anomalies in the midlatitude ocean are correlated with large-scale quasi-stationary atmospheric perturbations (Namias 1965; Namias and Cayan 1981; Wallace and Jiang 1987; Wallace et al. 1990; Wallace et al. 1992). The observed spatial relationships are consistent with the picture that the SST anomalies are primarily generated through local air–sea heat exchange (Cayan 1992b; 1992a). The three dimensional structure of wintertime atmospheric anomalies associated with interannual North Atlantic SST variability is shown in Fig. 1. This is done by compositing sea level pressure and 515-mb height fields associated with positive and negative SST anomalies, and calculating the difference between them. The composites are obtained using SST from U.K. Meteorological Office archives and atmospheric data from National Meteorological Center (NMC, now referred to as the National Centers for Environmental Prediction) analysis, for the months December–February. Zonal mean SST in the North Atlantic between 50° and 60°N is used to identify seasons with large positive and large negative anomalies [see Kushnir (1994) Table 1 for the list of contributing years].

The sea level pressure (SLP) pattern in Fig. 1a confirms the composite based on COADS data shown in Kushnir (1994). Positive and negative features in the anomalous SLP field (contours) straddle a warm SST region (shading). The weakened surface westerlies are consistent with a reduced heat loss by the ocean mixed

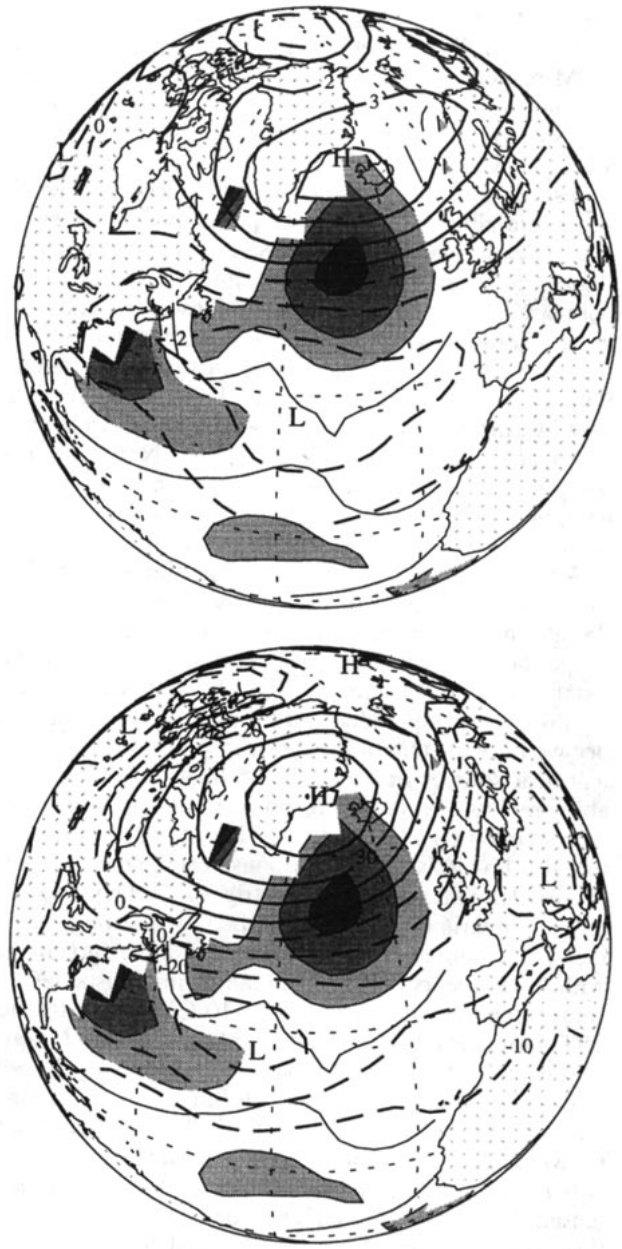

FIG. 1. Composite difference between winters (December–January) with moderate to large positive and negative North Atlantic SST anomalies in the latitude belt 50°–60°N. This difference emphasizes interannual variability [see Kushnir (1994) for more details]. Thick contoured fields are (a) sea level pressure and (b) 500-mb height; contour intervals 1 mb and 10 m, respectively; negative contours are dashed. The corresponding SST difference is depicted in shades of gray delineated by thin contour lines (dashed for negative values) at intervals of 0.2°C, zero contour omitted; the darker the shading; the larger the magnitude of the anomaly.

layer, hence a positive SST perturbation. In the Atlantic this situation also corresponds to reduced cold and dry outflow from the North American continent, hence weaker latent and sensible heat fluxes. A negative SST anomaly appears south of the positive anomaly, consistent with an atmospheric region of intensified westerlies, south of the center of the negative SLP anomaly (and in the Atlantic, a more intense invasion of continental air). Such ocean–atmosphere interaction appears to occur internally in the midlatitudes. In a recent study by Delworth (1996) similar Atlantic patterns were discerned in a coupled ocean–atmosphere GCM with clear evidence for the forcing of the SST anomalies by low-frequency variability internal to the midlatitude atmosphere.

The midlatitude atmospheric patterns associated with interannual variability in the SST field are equivalent barotropic, as illustrated by the 500-mb flow in Fig. 1b. The horizontal structure depicted by the midtropspheric field is similar to that of the SLP field. However, the amplitude of the atmospheric anomalies increase with height, implying *cold* lows and *warm* highs near the surface. This is the dominant vertical structure of atmospheric low-frequency variability with fixed boundary conditions (Lau 1981) and that of the extratropical response to tropical heating (Hoskins and Karoly 1981; Lau 1985). Therefore, the simplest hypothesis regarding interannual ocean–atmosphere interaction would be that atmospheric anomalies that exist independent of extratropical SST variability force the ocean with little feedback. But as outlined above, some GCM evidence, although mixed, suggests that these equivalent barotropic structures can be forced or modified by the local SST. If these GCM results are relevant to the real atmosphere, midlatitude ocean–atmosphere interaction may entail a positive feedback that will give rise to increased persistence of such anomalies as suggested, for example, by Deser and Blackmon (1993).

Kushnir (1994) compares interannual and interdecadal SST variability in the North Atlantic and concludes that ocean–atmosphere association on interdecadal timescales is different. That study compares the North Atlantic SST distribution and atmospheric circulation in two 15-yr periods, one with relatively warm SST north of 30°N (1950–64), and one with cold SST there (1970–84). Averaging the warm and cold years' December to May values, and determining the difference between the two, Kushnir (1994) finds an anomalous surface low centered at 45°N and 35°W, southeast of the warmest SST values (Fig. 9 there). In Fig. 2a we confirm these results using U.K. Meteorological Office SST data and NMC analysis. Over the Atlantic the composite displays an anomalous negative SLP region centered to the east of a positive SST anomaly that, while weaker than the interannual anomaly, is statistically significant (see Kushnir 1994). The relationship between the SST and SLP anomalies is clearly different

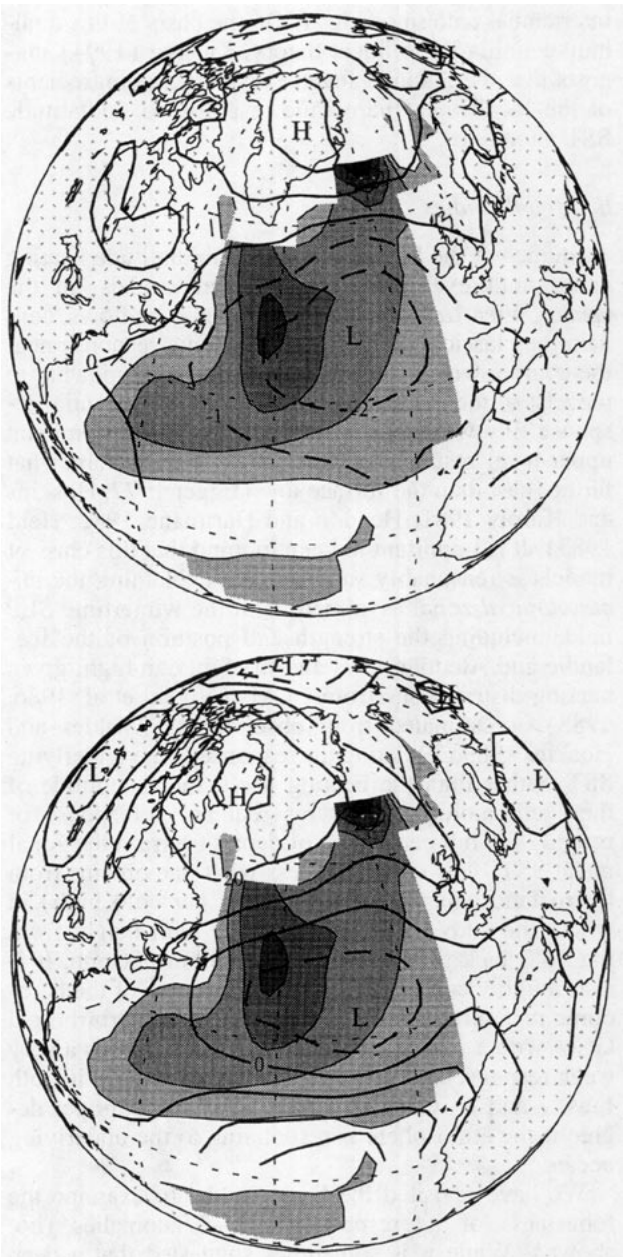

FIG. 2. As in Fig. 1 but for the difference between the cold seasons (December–April) of 1950–1964 and 1970–1984. This difference emphasizes interdecadal variability [see Kushnir (1994) for more details].

than in the interannual composite above (Fig. 1). At the 500-mb level (Fig. 2b, see also Shabbar et al. 1990) the midlatitude low pressure anomaly is still evident, but its amplitude is considerably weaker (SLP data imply a 1000-mb anomaly of about 25 m compared to a 15-m anomaly at 500 mb), and t statistics (not shown) indicate that it is no longer significant. This suggests a *warm* surface low and possibly a forced atmospheric response to SST. The situation is different from the

interannual pattern of Fig. 1. On the basis of this qualitative similarity to linear theory, Kushnir (1994) suggests that the Atlantic feature displays the ingredients of the local linear baroclinic response to midlatitude SST anomalies.

b. *Model studies*

Studies of the linear response to midlatitude heating using multilevel primitive equation models on the sphere, linearized about zonally symmetric flows, confirm the classical picture of a baroclinic response near the source, with a surface low displaced somewhat to the east of the maximum heating. The geopotential response tilts westward with height, with the dominant upper-level response being a high, placed somewhat farther east than the surface low (Egger 1977; Hoskins and Karoly 1981; Hendon and Hartmann 1982; Held 1983). It is important to keep in mind that this class of models is reasonably successful in explaining the *climatological* zonal asymmetries in the wintertime SLP field, including the strength and position of the Icelandic and Aleutian lows and the Siberian high, given heating distributions from GCMs (Nigam et al. 1986, 1988) or estimated from observations (Valdes and Hoskins 1989). Relating the response to the underlying SST, rather than the heating itself, the magnitude of these climatological features requires a response of roughly 0.5 mb per degree of departure from the zonal mean SST. This is more or less what one obtains from hydrostatic balance for a heat low (or cold high) in which the eddy temperature decays with height from the SST back to the zonal mean within 500 mb. It is also roughly consistent with the amplitude of the baroclinic response that Ting (1991) finds by perturbing a GCM with a zonally symmetric climate. This is a very weak response as compared with the anomalies in both Figs. 1 and 2, which require several millibars per degree if the atmosphere is responding to the underlying ocean.

We have revisited the linear model to examine the robustness of its response to SST anomalies (not shown). While it is sometimes suggested that a deep heat source, associated with latent heating in the storm tracks, will cause a qualitatively different response than shallow heating due to surface fluxes (i.e., Palmer and Sun 1985), we have not found this to be the case. Although the height at which the geopotential response changes sign near the source can be modified (see also Hendon and Hartmann 1982), the horizontal structure of the response is hardly affected. In the extreme case of an elevated heat source, one finds a barotropic response beneath the source, with westward tilt in and above the heated region, but there is still a low beneath and to the east of the source. A heating anomaly of this type would be produced in the (unlikely) circumstance that the depth of the heat source were increased without changing its strength at low levels. This would be one way of generating a pattern similar to that in Fig. 2, but it is just as difficult to explain the amplitude of the atmospheric anomaly in this way as with shallow heating.

3. Model and experiments

Two versions of a coarse-resolution GCM were used in this study. One model version included a full representation of the earth topography and land–sea contrast. This version will be referred to hereafter as the realistic GCM. In the other model version, an all-ocean surface at mean sea level was prescribed at the lower boundary. This version will be referred to hereafter as the idealized GCM.

Both GCMs are spectral with a rhomboidal truncation at wavenumber 15. In the vertical, the models have nine unequally spaced sigma levels, three of which are between the lower surface and the σ level at 0.83. The model physics include surface exchange of momentum, heat, and moisture, expressed in terms of the bulk aerodynamics formulas, with a drag coefficient that depends only on the surface type (land or ocean), and a moist convective adjustment scheme.

The realistic GCM incorporates a cloud prediction scheme by Wetherald and Manabe (1988). As in Kushnir and Lau (1992), the model is run with the solar zenith angle fixed throughout the integration (perpetual mode). January and October zenith angles are prescribed in two sets of integrations to examine the effect of the changing atmospheric condition, in particular the strength of the westerlies, on the response. The background SST field and sea ice distribution as well as soil moisture and land snow cover are also held fixed in the appropriate monthly mean values, taken from a previous model integration that incorporated the full annual cycle. The long-term Northern Hemisphere average of the unperturbed model integration with January conditions is presented in Fig. 3. Note that the North Atlantic is influenced by a steep meridional sea level pressure gradient (Fig. 3a), under the exit region of the North American jet stream (Fig. 3b). Surface wind speed over the SST anomaly region is 6–8 m s^{-1}, in reasonable agreement with observations. The October low and high sea level pressure centers, as well as the Atlantic jet stream, retain their January position. However, the October surface pressure gradient over the North Atlantic is only one-half as strong as in January and the upper-level jet is also considerably weaker.

The idealized version of the model is identical to the model used by Ting (1991). This version of the model prescribes a zonally symmetric cloud climatology in its radiative transfer calculations. As in Ting (1991), the idealized model has an all ocean lower surface with prescribed SST. In this experiment, however, the idealized SST field was modified to include a large zonal asymmetry, introduced in order to induce a stationary, planetary-scale perturbation in the atmospheric flow. The SST asymmetry is produced by a Gaussian-shaped

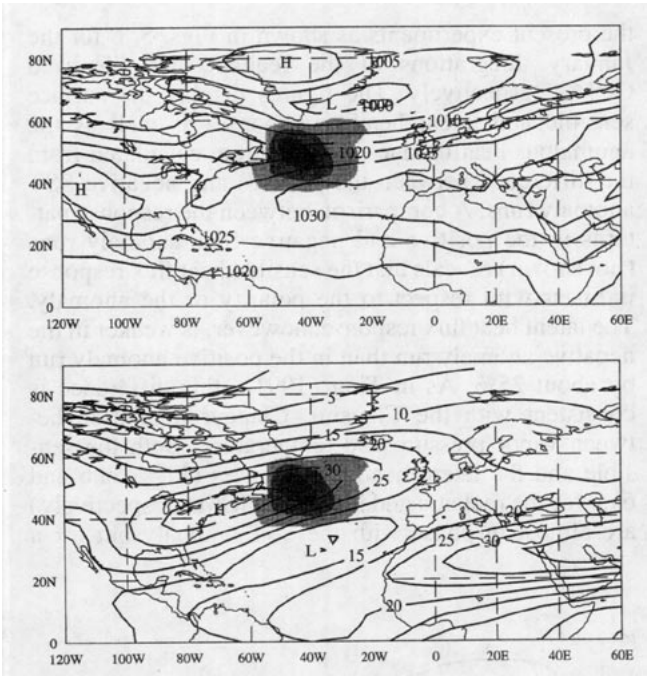

FIG. 3. Long-term mean of the realistic GCM perpetual January integration: (a) sea level pressure, (b) 205-mb zonal wind. The prescribed SST anomaly is depicted by shading at interval of 1°C, beginning at 1°C. Contour interval is 5 mb for sea level pressure and 5 m s^{-1} for zonal wind.

cold anomaly centered at 65°N with a minimum value of −45°C. These cold temperatures are clearly not meant to correspond to oceanic temperatures, but rather to the wintertime surface temperature over Siberia.

The idealized model was run with fixed mid-January solar zenith angle. The model mean sea level pressure field and zonal wind distribution at 205 mb are as shown in Figs. 4a,b respectively. These fields display high pressure over the cold dome, an elongated low with a weak southwest to northeast tilt over the warm surface, and a localized jet stream maximum in the midlatitudes. This situation resembles the climatological flow of the realistic GCM over the North Atlantic (Fig. 3) except that the zonal scale of the stationary features is larger than that in the realistic GCM. Here too the mean surface wind speed over the SST anomaly region reached values of 6–8 m s^{-1}.

Both GCMs were forced with a monopolar SST anomaly in the jet exit region, as depicted by the shaded areas in Figs. 3, 4. To enhance the signal-to-noise ratio, an SST anomaly larger than observed, with a maximum value of 4°C, was prescribed. An anomaly of similar magnitude was used by Palmer and Sun (1985). The SST anomaly, and its negative counterpart, were added to the climatological SST distribution to test the dependence of the response on the polarity of the perturbation. The anomaly in the realistic GCM experiment was located in the western North Atlantic, centered at 50°N and 40°W. In the idealized GCM the anomaly was located at 40°N and 60°W. The horizontal scale of the SST anomaly prescribed in the idealized mode is twice as large as that of the realistic GCM, consistent with the larger scales of the zonal asymmetry in the former. In both models the anomaly is under the influence of maximum surface westerlies and just downstream of the maximum in baroclinic eddy activity. All the experiments described below were integrated for 6000 days with fixed forcing to allow the study of the models' equilibrium response to the SST anomaly. Unperturbed (control) integrations of comparable length were also performed.

The results of the experiment are presented in terms of half the difference between the means of the positive and negative anomaly runs. We find that asymmetry with respect to the polarity of the SST anomaly (i.e., differences between the response to positive SST anomalies and the response to negative anomalies), particularly in the idealized model, is a second-order effect and will hereafter be referred to only when relevant. To assess the statistical significance of the results, a t variable was calculated as in Pitcher et al. (1988) and Kushnir and Lau (1992). However, to preserve the clarity of the figures, statistical significance test results are not shown. Unless noted otherwise, all features discussed below were found to be statistically significant at or above the 95% level.

4. The structure of thermal forcing in model integrations

In his review of midlatitude ocean–atmosphere interaction Frankignoul (1985) noted that the relationship between the SST anomaly and the related heating anomaly in the atmosphere can be rather complex. This was partially supported by the precipitation anomaly fields in Lau and Nath (1990) and Kushnir and Lau (1992). However Palmer and Sun (1985) and Ting (1991) presented evidence that the heating fields are in phase with the SST anomaly. This is also the case in

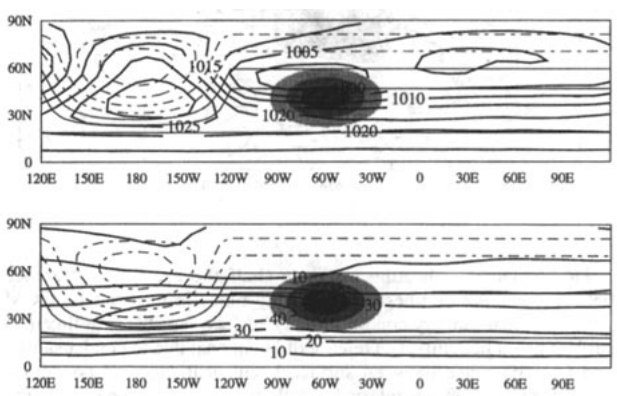

FIG. 4. As in Fig. 3 but for the idealized GCM. The distribution of mean surface temperature was added to the figure; it is depicted by thin contours at intervals of 10°C, dashed for negative values.

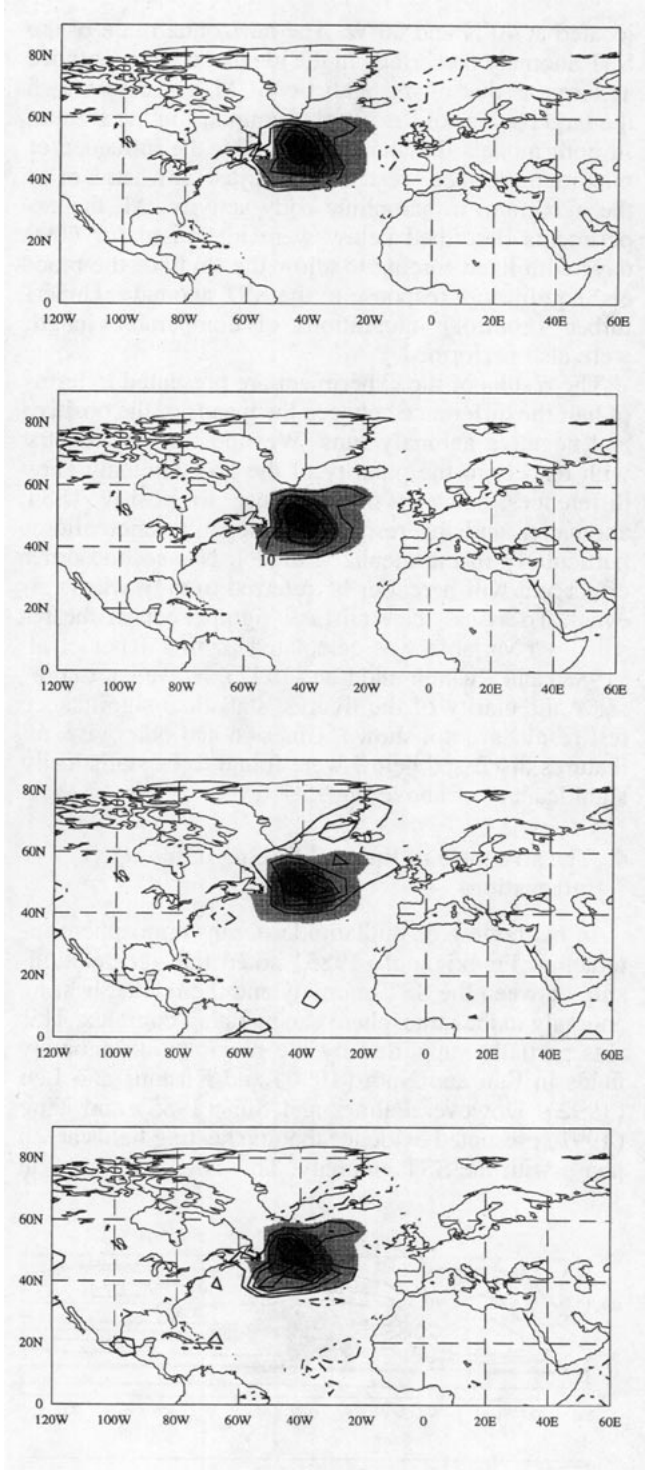

FIG. 5. Diabatic heating response (half the averaged difference between positive and negative anomaly runs) in the realistic GCM with perpetual January conditions. (a) Surface sensible heat flux, (b) surface latent heat flux, (c) release of latent heat due to condensation, and (d) difference between surface latent heat flux and condensational heating. Contour interval is 5 W m^{-2} except for (b) where the contour interval is doubled; negative contours are dashed. The zero contour is omitted for clarity. Shading depicts the prescribed SST anomaly as in Fig. 3.

the present experiments as shown in Figs. 5, 6 for the January integrations of the realistic and idealized GCMs, respectively. The figures display the surface sensible and latent heating response, as well as the anomalous heating due to convection, calculated from the difference between the positive and negative SST anomaly runs. A comparison between the response patterns in the positive and negative SST anomaly runs (not shown) reveals that the sensible heat flux response is linear with respect to the polarity of the anomaly. The latent heat flux response, however, is weaker in the negative anomaly run than in the positive anomaly run by about 25%. As in Ting (1991), this difference is consistent with the Clausius–Clapeyron relation between vapor pressure and temperature. Both the sensible and the latent heating responses (Figs. 5a,b and 6a,b for the realistic and idealized GCMs, respectively) are almost in phase with the SST anomaly but for a

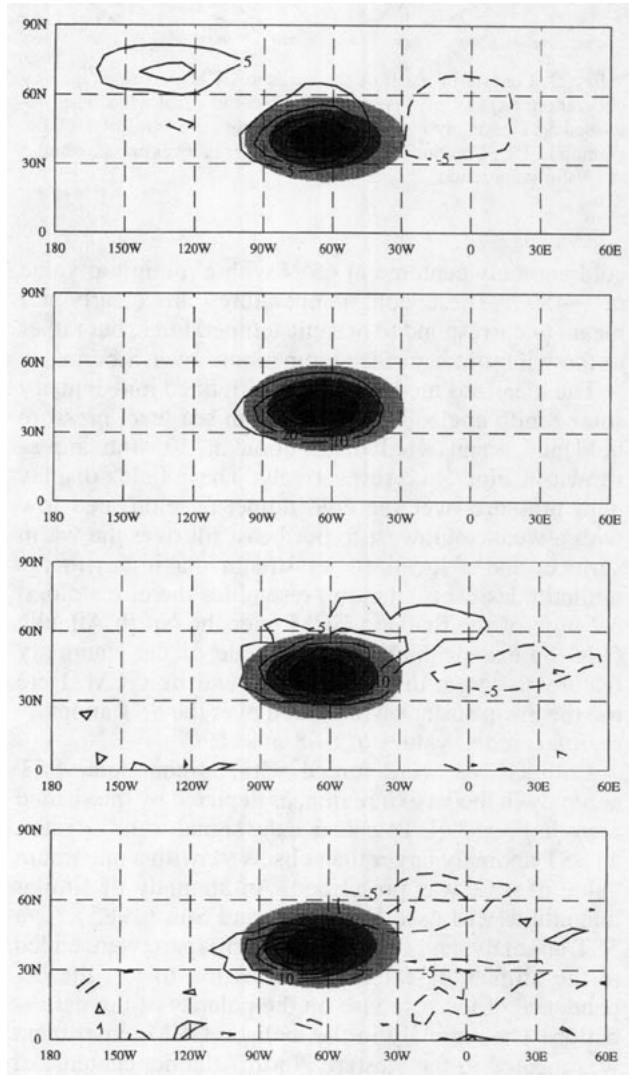

FIG. 6. As in Fig. 5 but for the idealized GCM.

small shift upstream, most clearly seen in the sensible heat flux field. This result (also consistent with the findings of Ting) seems to reflect the adjustment of the boundary layer to the change in underlying SST as the air moves over the anomaly. Note also the similarity between the realistic GCM and the idealized model in the magnitude of the surface heat exchange anomaly and its relation to the SST anomaly.

Only about one-half of the surface latent heat flux is realized as local atmospheric heating; the rest is exported to other regions. This is clear from the response pattern in the precipitation field, presented here as the equivalent amount of heat released by condensation (Figs. 5c, 6c for the realistic and idealized GCM, respectively). The convective heating anomaly is close to being in phase with the SST anomaly, unlike the results obtained in the Pacific experiment of Kushnir and Lau (1992) but similar to Ting (1991). The shift in precipitation with respect to the SST anomaly is emphasized in the evaporation minus precipitation ($E - P$) fields (Figs. 5d, 6d for the idealized and realistic GCMs, respectively; note that despite the impression gained from these figures, because of the emphasis on the local response, the global average of $E - P$ fields is zero).

The perpetual October integration (not shown) displays a similar in-phase relationship between surface fluxes and condensation on one hand, and the SST anomaly on the other hand. The October sensible heat flux response is 20% weaker than the January response but evaporation remains similar. These differences are consistent with weaker surface winds, the reduction in the air–sea temperature contrast, but higher SST values, in the October simulation.

The net anomalous local heating due to sensible heat flux and evaporation is thus realized mostly in phase with the anomaly. Overall, turbulent surface fluxes would act to attenuate the SST anomaly. Had any ocean atmosphere interaction been allowed, this heat exchange would have dissipated an SST anomaly of the present magnitude in a mixed layer 50-m deep in about 100 days.

The realistic GCM and idealized model differ in their treatment of clouds. The idealized model uses fixed zonally symmetric clouds in the radiative calculations and as such shows very little response in the fields of radiative heating. The realistic GCM attempts to predict clouds. Over the SST anomaly, cloudiness increases (decreases) by 20%–25% as SST is increased (decreased) with respect to climatology. This leads to the radiative cooling (warming) of the lowest model layer over the warm (cold) SST anomaly, an effect that offsets roughly 25% of the sensible heat warming (cooling) of that layer. In the absence of a cloud parameterization (e.g., in the idealized run), moist convective adjustment balances the entire amount due to sensible heating (cooling) of the lowest model layer, resulting in a deeper tropospheric distribution of heat and moisture. It appears that by balancing part of the sensible heating (cooling) clouds reduce the intensity of the convective upward penetration of heat and moisture, and the response to midlatitude SST anomalies weakens. This effect does not seem to be realistic. In fact, in the climatological sense cloud amount seems to be inversely proportional to SST [compare the January east–west distribution of cloudiness to that of SST in the North Atlantic as given, e.g., in Esbensen and Kushnir (1981)]. A negative correlation between SST and low cloud amount was also reported by Norris and Leovy (1994) in their study of summer cloudiness over the North Pacific.

The vertical distribution of net anomalous heating rate in the realistic GCM with January and October insolation are depicted in Figs. 7a,b, respectively. Figure 8 is the corresponding idealized model result. These figures display a longitude height cross section through the center of the SST anomaly of the total heating response (in varying shades of gray) as well as the air temperature response (contours). The differences in

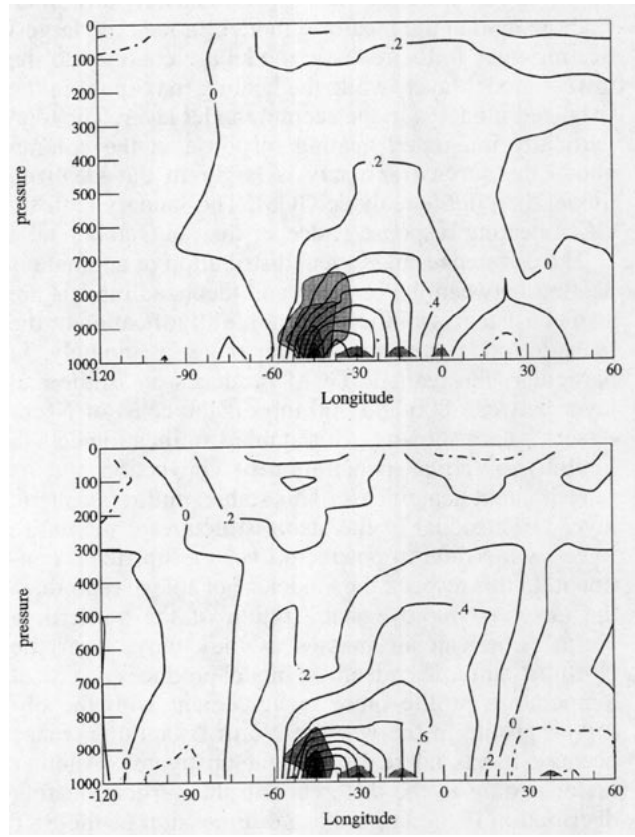

FIG. 7. Realistic GCM longitude–pressure cross section through center of SST anomaly (52°N) showing total diabatic heating rate (shades of gray delineated by thin contours) and temperature response (thick contours): (a) January conditions, (b) October conditions. Contour (and shading) interval is 0.5°C day^{-1} for heating, dashed contours delineate negative values, and zero contour is omitted. The temperature field is contoured with 0.2°C interval; negative contours are dashed.

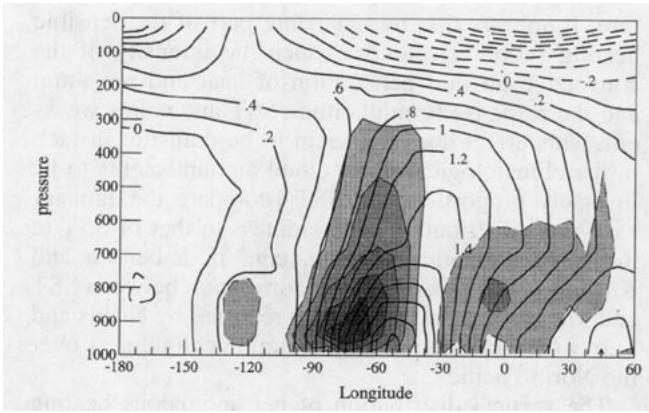

FIG. 8. As in Fig. 7 but for the idealized model. Cross section is at 43°N.

heating rate between the negative and positive anomaly runs (not shown) are subtle and stem from the differences in surface evaporation. The vertical distribution of heating in the realistic GCM is considerably more shallow than in the idealized model. In fact, the largest heating rates in the realistic model are confined to the lowest model layer, while the heating maximum in the idealized model is in the second model layer. The total vertically integrated heating response in the column above the surface anomaly is larger in the idealized model than in the realistic GCM. The January realistic GCM heating response is deeper than in October.

The differences in vertical distribution of anomalous heating between the realistic and idealized models are also consistent with the more stable stratification of the realistic model atmosphere over the SST anomaly. In particular, the realistic GCM produces an isothermal layer between 800 and 700 mb off the coast of North America (not shown). This stable stratification acts to inhibit the vertical penetration of convection and its related latent heat release. This stable, midtropospheric layer is a residual of the stable structure of the entire lower wintertime troposphere over the upstream continent. In this respect, the model is not able to reproduce the observed rapid destabilization of the wintertime North American air masses as they move over the North Atlantic. The idealized model produces a vertical temperature profile more in agreement with the observed profile in the western North Atlantic (perhaps because it has no real continent upstream). Another factor adding to the difference in the vertical heating distribution is the larger spatial dimension of the SST anomaly in the idealized model. This exposes the idealized model atmosphere to anomalous heating for a longer time as it is being advected eastward, allowing the heat to penetrate more deeply. We repeated the integration of the idealized model with an SST anomaly half the size of the one shown (and similar in size to the realistic GCM anomaly) and found that the vertical heating response decrease by a factor of 2, but its vertical penetration remains unchanged (not shown).

The vertical cross sections of the atmospheric temperature response in the realistic GCM with January and October insolation are depicted by contours in Figs. 7a,b, respectively, and for the idealized GCM in Fig. 8. Of the two realistic GCM integrations (Figs. 7a,b), the October run displays a stronger low-tropospheric temperature response. The idealized model response is considerably stronger and vertically deeper than in both realistic model runs (Fig. 8). These different temperature response patterns are consistent with the vertical distribution of diabatic heating in the different runs (Figs. 7, 8, shaded). The idealized model temperature response near the lower surface is close to 2.5°C, about 1° more than in the realistic GCM. The larger spatial scale of the anomaly specified in the idealized model evidently allows the atmosphere to equilibrate more fully with the SST change. The latter is also consistent with the small but similar difference between the October integration of the realistic GCM with its weak surface winds and the January integration with strong zonal advection that reduces the time of atmospheric exposure to the SST anomaly. When the idealized model is forced with an SST anomaly similar in magnitude but half the horizontal scale (not shown), the temperature response is weakened by a factor of 2 but is still larger than in the realistic GCM. In all cases, the temperature response is shifted eastward with respect to the heating anomaly, as expected from linear theory.

5. Geopotential height response

The vertical cross sections of geopotential height response are shown in Figs. 9, 10. The height responses are hydrostatically consistent with the temperature responses in Figs. 7 and 8. Thus, the October negative height response in the lower troposphere is stronger and less shallow than its January counterpart and is more similar to the lower-tropospheric response in the idealized model. The upper-level height responses in both the January and October runs of the realistic model are similar (Figs. 9a,b) and much weaker than in the idealized model (Fig. 10), consistent with the respective vertical penetration of the heating response.

Above the SST anomaly, the geopotential height distribution (Figs. 9, 10) displays a baroclinic vertical structure with a weak surface low in phase with the atmospheric temperature response (it is clearly to the east of the heating anomaly in the idealized model case). The height response changes polarity in the lower troposphere and intensifies to a maximum at the tropopause. The phase relationship between the surface low and the SST anomaly is such that meridional advection of the mean temperature field by an anomalous northerly wind component helps to balance the low-level heat source. The present temperature and geopotential height response patterns are consistent with

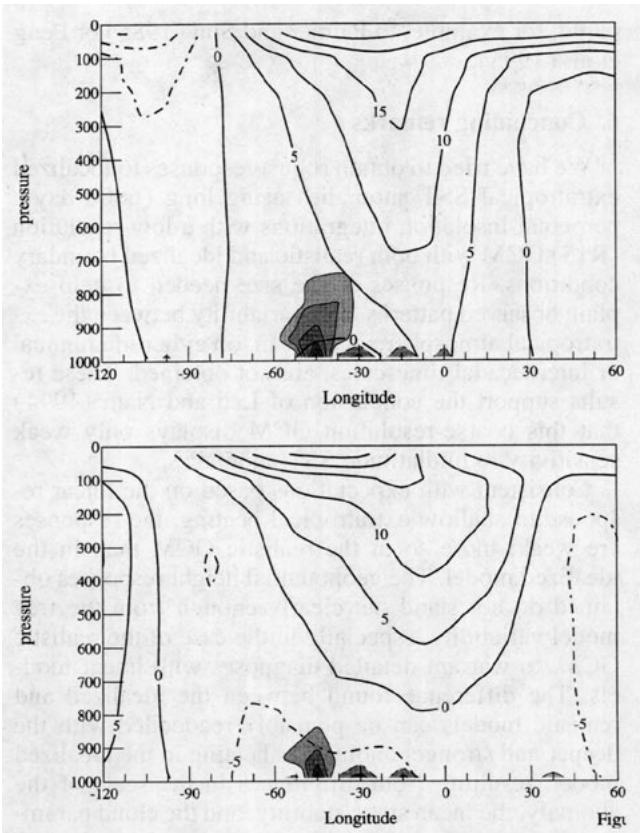

FIG. 9. Realistic GCM longitude–height cross section through the center of SST anomaly (52°N) showing the geopotential response (thick contours): (a) January conditions, (b) October conditions. Contour interval is 5 m; negative contours are dashed. Diabatic heating rate field is shaded as in Fig. 7.

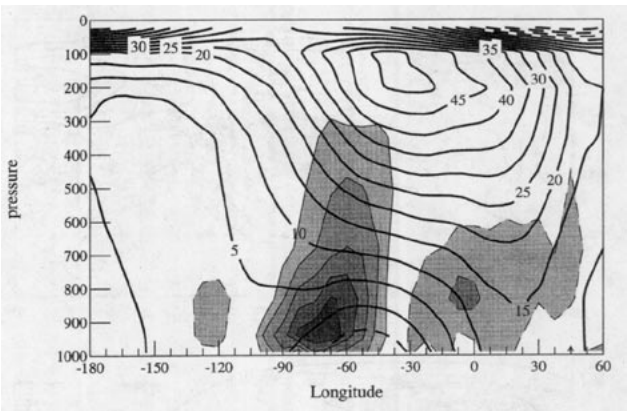

FIG. 10. As in Fig. 9 but for the idealized mode. Cross section is at 43°N.

the results of Ting (1991). Thus, zonal asymmetry in the unperturbed model climate did not result in a change in the vertical structure of the response.

The vertical cross section of the temperature and height response display a modest asymmetry with respect to the polarity of the SST anomaly. The temperature response to a negative SST anomaly is shallower and weaker than the response to a positive anomaly (not shown). This is consistent with the weaker anomalous latent heat release in the negative model runs, due initially to reduced evaporation.

The horizontal structure of the geopotential height response at 990 and 515 mb is shown in Figs. 11 and 12 for the realistic model in October and January conditions respectively, and Fig. 13 for the idealized model. The large differences among the figures is disappointing, given the 6000-day-long integrations. The idealized model response has a large zonally symmetric component that the realistic GCM does not produce. This response is robust, being clearly present with opposite signs in the positive and negative anomaly cases. This difference between the idealized and realistic GCMs is not related to the larger zonal extent of the anomaly prescribed in the idealized model. An integration with an SST anomaly of half the zonal scale yields a similar zonally elongated response. The zonally asymmetric component of the idealized GCMs response is also robust, and agrees qualitatively with the results of Ting (1991) and with linear theory, near the region of forcing. Forcing the idealized model with an anomaly of smaller zonal extent results in half as strong a response as in the case shown, but virtually of the

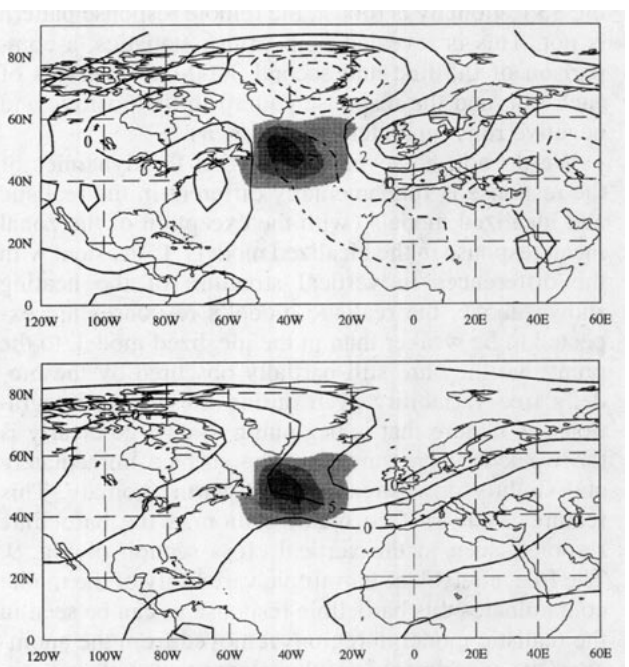

FIG. 11. Realistic GCM geopotential pressure response under January conditions: (a) 990 mb, (b) 515 mb. Contour interval is 2 m in (a) and 5 m in (b), (c). Negative contours are dashed. Gray shading depicts the prescribed SST anomaly with intervals of 1°C beginning at 1°C.

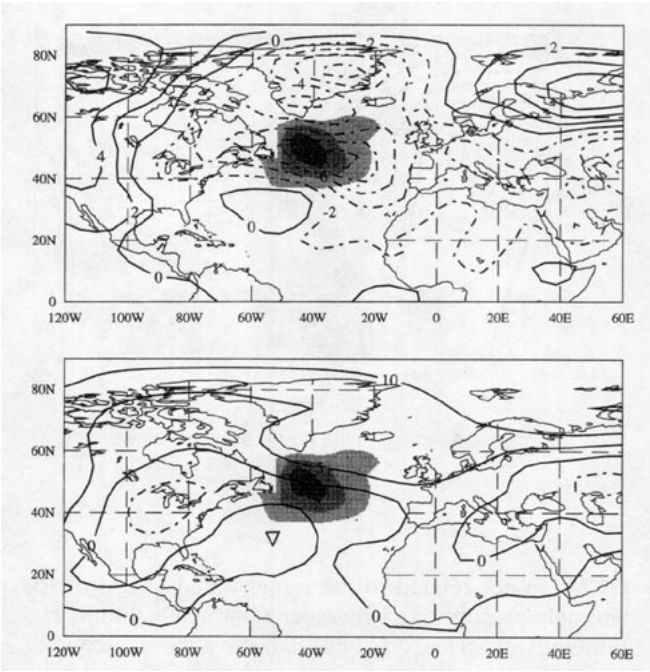

FIG. 12. As in Fig. 11 but for the realistic GCM in October conditions.

same structure. In contrast, while the general structure of the realistic GCM height response in the vicinity of the SST anomaly is robust, the remote response pattern is not. This is revealed both from t statistics, a comparison of the first and second 3000-day intervals of each run, and the response pattern in the positive and negative runs separately (not shown).

We do not, however, believe that the dynamics of the response is fundamentally different in the realistic and idealized models (with the exception of the zonal mean response in the idealized model). Consistent with the differences in vertical structure of the heating shown above, the realistic model's responses are expected to be weaker than in the idealized model, to the point that they are still partially obscured by the model's free variability even during these long integrations. A feature that is beginning to emerge clearly is the weak low pressure near the surface immediately and slightly downstream of the warm anomaly. This feature is the surface manifestation of the baroclinic response seen in the vertical cross section of Fig. 9. The free, equivalent-barotropic variability of the model contaminates this baroclinic response as can be seen in the realistic model in regions removed from the anomaly. Our experiments are thus consistent with a weak, "linear" baroclinic response to a midlatitude surface heat source, similar to Ting (1991). The equivalent barotropic part of the response in these integrations (downstream of the SST anomaly) is rather week compared, for example, to Palmer and Sun (1985) or Peng et al. (1995).

6. Concluding remarks

We have tried to obtain robust responses to localized extratropical SST anomalies using long (6000 day), perpetual-insolation integrations with a low-resolution (R15) GCM with both realistic and idealized boundary conditions. Responses of the size needed to help explain observed patterns of covariability between the extratropical atmosphere and ocean, on either interannual or interdecadal timescales, are not obtained. These results support the conclusion of Lau and Nath (1994) that this coarse-resolution GCM displays only weak sensitivity to midlatitude SST anomalies.

Consistent with expectations based on the linear response to shallow extratropical heating, the responses are weak: more so in the realistic GCM than in the idealized model. The geopotential height responses obtained do not stand out clearly enough from the free model variability, especially in the case of the realistic GCM, to warrant detailed diagnoses with linear models. The difference found between the idealized and realistic models can be plausibly reconciled with the deeper and stronger anomalous heating in the idealized model, resulting from differences in the scale of the anomaly, the mean static stability, and the cloud parameterization. As highlighted by this comparison, the factors controlling the depth of penetration of the heat anomaly, either directly or through the maintenance of the control climate static stability (such as the strength of the surface heat exchange, boundary layer mixing, and cloud–radiative interaction), are important for the strength of the response.

In all cases examined in the present study, the vertical structure of the response in the vicinity of the SST anomaly is baroclinic. A robust equivalent barotropic response is not observed. The R15 model's eddy momentum fluxes are known to be deficient by roughly a factor of two. If changes in these fluxes are important

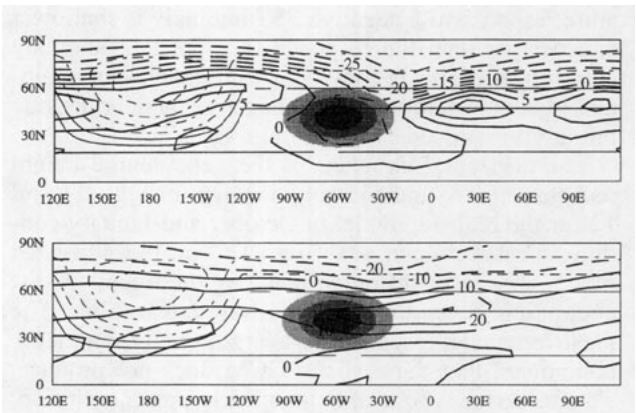

FIG. 13. As in Fig. 11 but for the idealized model. Thin contours depict the surface temperature field as in Fig. 4.

for the generation of equivalent barotropic atmospheric anomalies in response to SST anomalies, this model may not be capable of generating them with sufficient intensity. This needs to be explored further with models with higher resolution that offer a more realistic simulation of eddy momentum fluxes.

While there is no resemblance between the model responses and the atmospheric patterns associated with interannual variability (Fig. 1) there exists qualitative resemblance between the latter and the interdecadal pattern (Fig. 2). In the latter, the height anomaly in the lower troposphere bears a similar phase relationship to the SST anomalies found in the model experiments. If a relatively weak linear response is excited in the atmosphere, we expect to detect it only if it existed for a long enough time or occurred repeatedly for several consecutive winters, allowing the averaging needed to suppress the large internal variability. The equilibrium response of the model may thus be relevant for the study of long-term climate variability. However, for the GCM results to be applicable for North Atlantic interdecadal variability we must be able to explain the much larger amplitude of the observed anomalies in comparison to the simulated response. Also, although the observed anomalies appear to decay with height (Fig. 2), the model response decays much more rapidly and reverses sign by the midtroposphere. Both these deficiencies could possibly be simulated in a linear model, with a much deeper heating profile.

Present results are qualitatively consistent with results from other GCM experiments involving very large SST anomalies in the North Atlantic such as Rind et al. (1986) and Manabe and Stouffer (1988). These experiments were integrated in a realistic simulation of the seasonal cycle, thus lending credence to the assertion made in the introduction that equilibrium experiments in perpetual conditions are relevant to interpreting the more complicated case of a full annual cycle simulation. Note that the Rind et al. and Manabe and Stouffer atmospheric responses to changing SST in the North Atlantic are also qualitatively similar to the interdecadal variability in Fig. 2.

The present study adds to the controversy regarding the effect of midlatitude SST on climate variability. In this respect we note that a recent experiment with a coupled ocean–atmosphere GCM (Latif and Barnett 1994) displays a quasi-decadal ocean–atmosphere interaction in the North Pacific region with a strong equivalent barotropic atmospheric response to SST fluctuations. The continued disparity between different GCM results requires further study of midlatitude ocean–atmosphere interaction. Despite the tantalizing evidence from other models that barotropic responses can be obtained, there is not enough evidence that these modes are consistently reproducible [e.g., Peng et al. (1995) differences between positive and negative anomaly runs, and November and January conditions]. In light of this disparity in model simulations we continue to believe that it is important to try to isolate an equivalent barotropic response to midlatitude SST anomalies and examine the conditions necessary for its existence. Such study could best be achieved in an idealized setting but with a fully nonlinear model, for example, a GCM with an all-ocean lower boundary conditions with prescribed SST and fixed insolation. This will allow one to conduct a systematic investigation of the dependence of the response on the structure of the control climate, or the low-frequency variability of that climate, in ways that would lead to a better understanding of midlatitude ocean–atmosphere interaction.

Acknowledgments. This research was supported by NOAA Grant NA26GP0022. Comments by Drs. N.-C. Lau and T. Delworth on an earlier version of this manuscript are greatly appreciated. The authors would like to thank M. J. Nath, P. J. Phillipps, and A. Kaplan for their valuable help in model integration, and data handling and analysis.

REFERENCES

Branstator, G. W., 1992: The maintenance of low-frequency atmospheric anomalies. *J. Atmos. Sci.,* **49,** 1924–1945.

Cayan, D. R., 1992a: Latent and sensible heat flux anomalies over the northern oceans: Driving the sea surface temperature. *J. Phys. Oceanogr.,* **22,** 859–881.

——, 1992b: Latent and sensible heat flux anomalies over the northern oceans: The connection to monthly atmospheric circulation. *J. Climate,* **5,** 354–369.

Delworth, T., 1996: North Atlantic interannual variability in a coupled ocean–atmosphere model. *J. Climate,* in press.

——, S. Manabe, and R. J. Stouffer, 1993: Interdecadal variations of the thermohaline circulation in a coupled ocean–atmosphere model. *J. Climate,* **6,** 1993–2011.

Deser, C., and M. L. Blackmon, 1993: Surface climate variations over the North Atlantic Ocean during winter: 1900–1989. *J. Climate,* **6,** 1743–1753.

Egger, J., 1977: On the linear theory of the atmospheric response to sea surface temperature anomalies. *J. Atmos. Sci.,* **34,** 603–614.

Esbensen, S. K., and Y. Kushnir, 1981: The heat budget of the global ocean: An atlas based on surface marine observations. Climate Research Institute, Rep. No. 29, Oregon State University, Corvallis, OR, 27 pp. plus 188 plates.

Ferranti, L., F. Molteni, and T. N. Palmer, 1994: Impact of localized tropical and extratropical SST anomalies in ensembles of seasonal GCM integrations. *Quart. J. Roy. Meteor. Soc.,* **120,** 1613–1645.

Frankignoul, C., 1985: Sea surface temperature anomalies, planetary waves and air–sea feedback in midlatitudes. *Rev. Geophys.,* **23,** 357–390.

Gordon, A. L., S. E. Zebiak, and K. Bryan, 1992: Climate variability and the Atlantic Ocean. *Eos, Trans. Amer. Geophys. Union,* **73,** 161, 164–165.

Held, I. M., 1983: Stationary and quasi-stationary eddies in the extratropical atmosphere: Theory. *Large Scale Dynamical Processes in the Atmosphere,* R. P. Pearce and B. J. Hoskins, Eds., Academic Press, 127–168.

——, and P. J. Phillipps, 1993: Sensitivity of the eddy momentum flux to meridional resolution in atmospheric GCMs. *J. Climate,* **6,** 499–507.

——, S. W. Lyons, and S. Nigam, 1989: Transients and the extratropical response to El Niño. *J. Atmos. Sci.,* **46,** 163–174.

Hendon, H. H., and D. L. Hartmann, 1982: Stationary waves on a sphere: Sensitivity to thermal feedback. *J. Atmos. Sci.,* **39,** 1906–1920.

Hoskins, B. J., and D. Karoly, 1981: The steady linear response of a spherical atmosphere to thermal and orographic forcing. *J. Atmos. Sci.,* **38,** 1179–1196.

Kushnir, Y., 1994: Interdecadal variations in North Atlantic sea surface temperature and associated atmospheric conditions. *J. Climate,* **7,** 141–157.

——, and N.-C. Lau, 1992: The general circulation model response to a North Pacific SST anomaly: Dependence on time scale and pattern polarity. *J. Climate,* **5,** 271–283.

Latif, M., and T. P. Barnett, 1994: Causes of decadal climate variability over the North Pacific and North America. *Science,* **266,** 634–637.

Lau, N.-C., 1981: A diagnostic study of recurrent meteorological anomalies appearing in a 15-year simulation with a GFDL general circulation model. *Mon. Wea. Rev.,* **109,** 2287–2311.

——, 1985: Modeling the seasonal dependence of the atmospheric response to observed El Niños in 1962–1976. *Mon. Wea. Rev.,* **113,** 1970–1996.

——, and M. J. Nath, 1990: A general circulation model study of the atmospheric response to extratropical SST anomalies observed in 1950–79. *J. Climate,* **3,** 965–989.

——, and ——, 1994: A modeling study of the relative roles of tropical and extratropical SST anomalies in the variability of the global atmosphere–ocean system. *J. Climate,* **7,** 1184–1207.

Manabe, S., and R. J. Stouffer, 1988: Two stable equilibria of a coupled ocean–atmosphere model. *J. Climate,* **1,** 841–866.

Molteni, F., L. Ferranti, T. N. Palmer, and P. Viterbo, 1993: A dynamical interpretation of the global response to equatorial Pacific SST anomalies. *J. Climate,* **6,** 777–795.

Namias, J., 1965: Short period climatic fluctuations. *Science,* **147,** 696–706.

——, and D. R. Cayan, 1981: Large-scale air–sea interactions and short period climate fluctuations. *Science,* **214,** 869–876.

Nigam, S., I. M. Held, and S. W. Lyons, 1986: Linear simulation of the stationary eddies in a general circulation model. Part I: The no-mountain model. *J. Atmos. Sci.,* **43,** 2944–2961.

——, ——, and ——, 1988: Linear simulation of the stationary eddies in a general circulation model. Part II: The "mountain" model. *J. Atmos. Sci.,* **45,** 1434–1452.

Norris, J. R., and C. B. Leowy, 1994: Interannual variability in stratiform cloudiness and sea surface temperature. *J. Climate,* **7,** 1915–1925.

Palmer, T. N., and Z. Sun, 1985: A modeling and observational study of the relationship between sea surface temperature in the north west Atlantic and the atmospheric general circulation. *Quart. J. Roy. Meteor. Soc.,* **111,** 947–975.

Peng, S., L. A. Mysak, H. Ritchie, J. Derome, and B. Dugas, 1995: The difference between early and middle winter atmospheric response to sea surface temperature anomalies in the northwest Atlantic. *J. Climate,* **8,** 137–157.

Pitcher, E. J., M. L. Blackmon, G. T. Bates, and S. Munoz, 1988: The effect of North Pacific sea surface temperature anomalies on the January climate of a general circulation model. *J. Atmos. Sci.,* **45,** 172–188.

Rind, D., D. Peteet, W. Broecker, A. McIntyre, and W. Ruddiman, 1986: The impact of cold North Atlantic sea surface temperature on climate: Implication for Younger Dryas cooling (11–10 k). *Climate Dyn.,* **1,** 3–33.

Shabbar, A., K. Higuchi, and J. L. Knox, 1990: Regional analysis of Northern Hemisphere 50 kPa geopotential height from 1946 to 1985. *J. Climate,* **3,** 543–557.

Ting, M., 1991: The stationary wave response to a midlatitude SST anomaly in an idealized GCM. *J. Atmos. Sci.,* **48,** 1249–1275.

——, and N.-C. Lau, 1993: A diagnostic and modeling study of the monthly mean wintertime anomalies appearing in a 100-year GCM experiment. *J. Atmos. Sci.,* **50,** 2845–2867.

Valdes, P. J., and B. J. Hoskins, 1989: Linear stationary wave simulations of the time-mean climatological flow. *J. Atmos. Sci.,* **46,** 2509–2527.

Wallace, J. M., and Q.-R. Jiang, 1987: On the observed structure of interannual variability of the atmosphere/ocean climate system. *Atmospheric and Oceanic Variability,* H. Cattle, Ed., Royal Meteorological Society, 17–43.

——, C. Smith, and Q.-R. Jiang, 1990: Spatial patterns of atmosphere/ocean interaction in the northern winter. *J. Climate,* **3,** 990–998.

——, ——, and C. S. Bretherton, 1992: Singular value decomposition of wintertime sea surface temperature and 500-mb height anomalies. *J. Climate,* **5,** 561–576.

Wetherald, R. T., and S. Manabe, 1988: Cloud feedback processes in a general circulation model. *J. Atmos. Sci.,* **45,** 1397–1415.